

## First Results on Angular Distributions of Thermal Dileptons in Nuclear Collisions

R. Arnaldi,<sup>1</sup> K. Banicz,<sup>2,3</sup> J. Castor,<sup>4</sup> B. Chaurand,<sup>5</sup> C. Cicalò,<sup>6</sup> A. Colla,<sup>1</sup> P. Cortese,<sup>1</sup> S. Damjanovic,<sup>2,3</sup> A. David,<sup>2,7</sup> A. de Falco,<sup>6</sup> A. Devaux,<sup>4</sup> L. Ducroux,<sup>8</sup> H. En'yo,<sup>9</sup> J. Fargeix,<sup>4</sup> A. Ferretti,<sup>1</sup> M. Floris,<sup>6</sup> A. Förster,<sup>2</sup> P. Force,<sup>4</sup> N. Guettet,<sup>2,4</sup> A. Guichard,<sup>8</sup> H. Gulkanian,<sup>10</sup> J. M. Heuser,<sup>9</sup> M. Keil,<sup>2,7</sup> L. Kluberg,<sup>2,5</sup> C. Lourenço,<sup>2</sup> J. Lozano,<sup>7</sup> F. Manso,<sup>4</sup> P. Martins,<sup>2,7</sup> A. Masoni,<sup>6</sup> A. Neves,<sup>7</sup> H. Ohnishi,<sup>9</sup> C. Oppedisano,<sup>1</sup> P. Parracho,<sup>2</sup> P. Pillot,<sup>8</sup> T. Poghosyan,<sup>10</sup> G. Puddu,<sup>6</sup> E. Radermacher,<sup>2</sup> P. Ramalhete,<sup>2</sup> P. Rosinsky,<sup>2</sup> E. Scomparin,<sup>1</sup> J. Seixas,<sup>7</sup> S. Serci,<sup>6</sup> R. Shahoyan,<sup>2,7</sup> P. Sonderegger,<sup>7</sup> H. J. Specht,<sup>3</sup> R. Tieulent,<sup>8</sup> G. Usai,<sup>6</sup> R. Veenhof,<sup>2</sup> and H. K. Wöhri<sup>6,7</sup>

(NA60 Collaboration)

<sup>1</sup>Università di Torino and INFN, Italy

<sup>2</sup>CERN, 1211 Geneva 23, Switzerland

<sup>3</sup>Physikalisches Institut der Universität Heidelberg, Germany

<sup>4</sup>LPC, Université Blaise Pascal and CNRS-IN2P3, Clermont-Ferrand, France

<sup>5</sup>LLR, Ecole Polytechnique and CNRS-IN2P3, Palaiseau, France

<sup>6</sup>Università di Cagliari and INFN, Cagliari, Italy

<sup>7</sup>Instituto Superior Técnico, Lisbon, Portugal

<sup>8</sup>IPN-Lyon, Université Claude Bernard Lyon-I and CNRS-IN2P3, Lyon, France

<sup>9</sup>RIKEN, Wako, Saitama, Japan

<sup>10</sup>YerPhI, Yerevan Physics Institute, Yerevan, Armenia

(Received 16 December 2008; published 5 June 2009)

The NA60 experiment at the CERN Super Proton Synchrotron has studied dimuon production in 158A GeV In-In collisions. The strong excess of pairs above the known sources found in the complete mass region  $0.2 < M < 2.6$  GeV has previously been interpreted as thermal radiation. We now present first results on the associated angular distributions. Using the Collins-Soper reference frame, the structure function parameters  $\lambda$ ,  $\mu$ , and  $\nu$  are measured to be zero, and the projected distributions in polar and azimuth angles are found to be uniform. The absence of any polarization is consistent with the interpretation of the excess dimuons as thermal radiation from a randomized system.

DOI: 10.1103/PhysRevLett.102.222301

PACS numbers: 25.75.-q, 12.38.Mh, 13.85.Qk

Lepton pairs are a particularly attractive observable to study the hot and dense matter created in high-energy nuclear collisions. Their continuous emission, undisturbed by final-state interactions, probes the entire space-time evolution of the fireball, including the early phases with the conjectured QCD phase transitions of chiral symmetry restoration and parton deconfinement. To the extent that the bulk constituents of the expanding matter (hadrons and partons) equilibrate, the direct lepton pairs generated by them are commonly referred to as “thermal radiation.” Our previous work has indicated “thermal” dilepton production to be largely mediated for  $M < 1$  GeV by  $\pi^+ \pi^-$  annihilation via the strongly broadened vector meson  $\rho$  [1], and for  $M > 1$  GeV by partonic processes like  $q\bar{q}$  annihilation [2,3]. The two dilepton variables basically explored in this work were mass  $M$  and transverse momentum  $p_T$ , where the correlations between the two were decisive in bearing out the nature of the emission sources in the two mass regions [2,3].

Further information on the production mechanism and the distribution of the annihilating particles, complementary to that from  $M$  and  $p_T$ , can be obtained from the study

of dilepton angular distributions. This Letter presents the first measurement of full dilepton angular distributions in the field of high-energy nuclear collisions. It is restricted to the mass region  $M < 1$  GeV, due to the lack of sufficient statistics for  $M > 1$  GeV. The question asked is simple: can one get direct experimental insight into whether the radiating matter is *thermalized*?

Historically, the interest in angular distributions of continuum lepton pairs was mostly motivated by the study of the Drell-Yan mechanism, following, in particular, the insight that the “naïve” QED interpretation [4] had to be significantly modified due to QCD effects [5–8]. The differential decay angular distribution in the rest frame of the virtual photon with respect to a suitably chosen set of axes, ignoring the rest mass of the leptons, can quite generally be written as

$$\frac{1}{\sigma} \frac{d\sigma}{d\Omega} \propto \left( 1 + \lambda \cos^2 \theta + \mu \sin 2\theta \cos \phi + \frac{\nu}{2} \sin^2 \theta \cos 2\phi \right). \quad (1)$$

The angular dependence on polar angle  $\theta$  and azimuth angle  $\phi$  dates back to [9], but the specific coefficients  $\lambda$ ,  $\mu$

and  $\nu$ , the “structure function” parameters, follow the nomenclature in, e.g., [8,10]. They are directly related to the helicity structure functions  $W_i$  defined in [6], and, in particular, to the spin density matrix  $R_{ij}^{\gamma^*}$  of the virtual photon  $\gamma^*$ , the main object of the spin analysis [7,10,11]. We have chosen here the Collins-Soper (CS) reference frame [5], where the quantization axis  $\vec{z}$  is defined as the bisector between the beam and negative target momenta  $\vec{p}_{\text{beam}}$  and  $-\vec{p}_{\text{target}}$ , which define the reaction plane. The polar angle  $\theta$  is then the angle between the momentum of the positive muon  $\vec{p}_{\mu^+}$  and the  $\vec{z}$  axis, which define the decay plane, while the azimuth angle  $\phi$  is the angle between the reaction and the decay planes. However, the particular choice of the frame is not really relevant here, since the determination of the full set of coefficients  $\lambda$ ,  $\mu$  and  $\nu$  allows to compute them in any other frame by a simple transformation [8]. This would not apply if only the  $\cos\theta$  distribution would be measured.

In principle, the dilepton angular distributions can be anisotropic, with all structure function parameters  $\lambda$ ,  $\mu$ ,  $\nu \neq 0$  [5–8,10]. Even for spinless particles in the initial state like in  $\pi^+\pi^-$  annihilation, the parameters can still have any value  $\neq 0$ , since the spin density matrix of the virtual photon also receives contributions from orbital angular momentum [12]. Very elementary examples are  $q\bar{q}$  and  $\pi^+\pi^-$  annihilation along the beam direction for  $p_T = 0$ . Here  $\mu = \nu = 0$  and  $\lambda = +1$  for  $q\bar{q}$  (like the lowest order DY mechanism [4]) and  $\lambda = -1$  for  $\pi^+\pi^-$  [12], corresponding to transverse and longitudinal polarization of the virtual photon, respectively. However, a completely random orientation of annihilating partons or pions in three dimensions (but not in two [11]) would lead to  $\lambda, \mu, \nu = 0$  [11–13], and that is the case of prime interest here.

Details of the NA60 apparatus are contained in [3,14]. The data sample for 158A GeV In-In collisions is the same as used in [1,2], and the different analysis steps follow the same sequence: assessment of the combinatorial background from  $\pi$  and  $K$  decays by a mixed-event technique, assessment of the fake matches (associations of muons to nonmuon vertex tracks in the Si pixel telescope), isolation of the dimuon excess by subtraction of the known meson decay sources and charm from the net opposite-sign sample, and finally correction for acceptance and pair efficiency. All steps are now done independently in each  $[\frac{dN}{d\cos\theta d\phi}]_{ij}$  bin. The binning is varied depending on the goal, thereby assuring that the results are stable with respect to the bin widths chosen.

The assessment of the two background sources and open charm is extensively discussed in Ref. [3]. The centrality-integrated net mass spectrum after background subtraction is shown in Fig. 1 together with the contributions from neutral meson decays: the 2-body decays of the  $\eta$ ,  $\omega$  and  $\phi$  resonances, and the Dalitz decays of the  $\eta$ ,  $\eta'$  and  $\omega$ . The data clearly exceed the sum of the decay sources. The

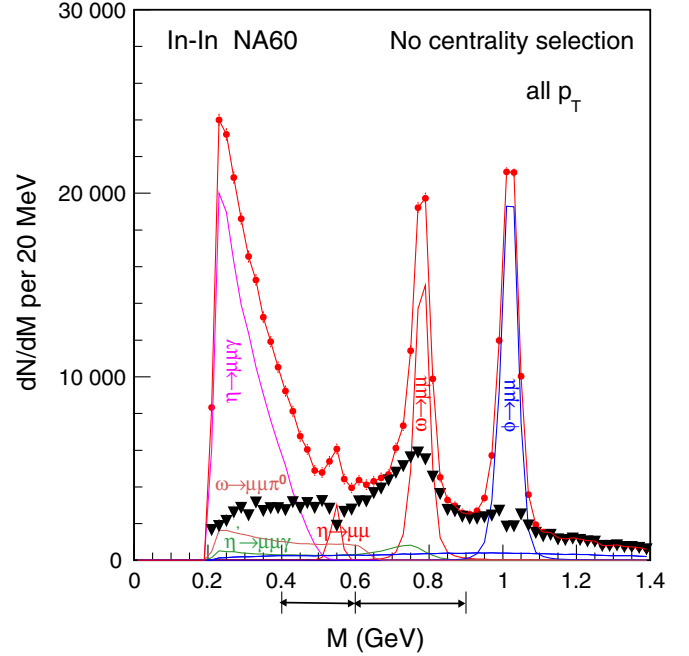


FIG. 1 (color online). Isolation of an excess above the electromagnetic decays of neutral mesons (see text). Total data (closed circles), individual cocktail sources (solid lines), difference data (thick triangles), sum of cocktail sources and difference data (line through the closed circles). Open charm still contained.

excess dimuons are isolated by subtracting them from the total (except for the  $\rho$ ), based solely on *local* criteria [1,2]. The excess for  $M < 1$  GeV is interpreted as the strongly broadened  $\rho$  which is continuously regenerated by  $\pi^+\pi^-$  annihilation [1,2]. Two adjacent mass windows indicated in Fig. 1 are used for the subsequent angular distribution analysis: the  $\rho$ -like region  $0.6 < M < 0.9$ , and the low-mass tail  $0.4 < M < 0.6$  GeV. To exclude the region of the low- $m_T$  rise seen for all masses [2], a transverse momentum cut of  $p_T > 0.6$  GeV is applied, leaving about 54 000 excess pairs in the two mass windows. The subtracted data for the  $\omega$  and  $\phi$ , about 73 000 pairs, are subject to the same further analysis steps as the excess data and are used for comparison.

The correction for the acceptance of the NA60 apparatus requires, in principle, a five-dimensional grid in  $M - p_T - y - \cos\theta - \phi$  space. To avoid large statistical errors in low-acceptance bins, the correction is performed in two-dimensional  $\cos\theta - \phi$  space, using the measured data for  $M$ ,  $p_T$  [2] and  $y$  [15] as an input to the Monte Carlo (MC) simulation of the  $\cos\theta - \phi$  acceptance matrix. The sensitivity of the final results to variations of this  $M - p_T - y$  input has been checked, and the effects are found to be considerably smaller than the statistical errors of the results. The MC simulations were done in an overlay mode with real data to include the effects of pair reconstruction efficiencies. The product acceptance  $\times$  efficiency is illustrated in Fig. 2 for  $0.6 < M < 0.9$  GeV and  $p_T > 0.6$  GeV.

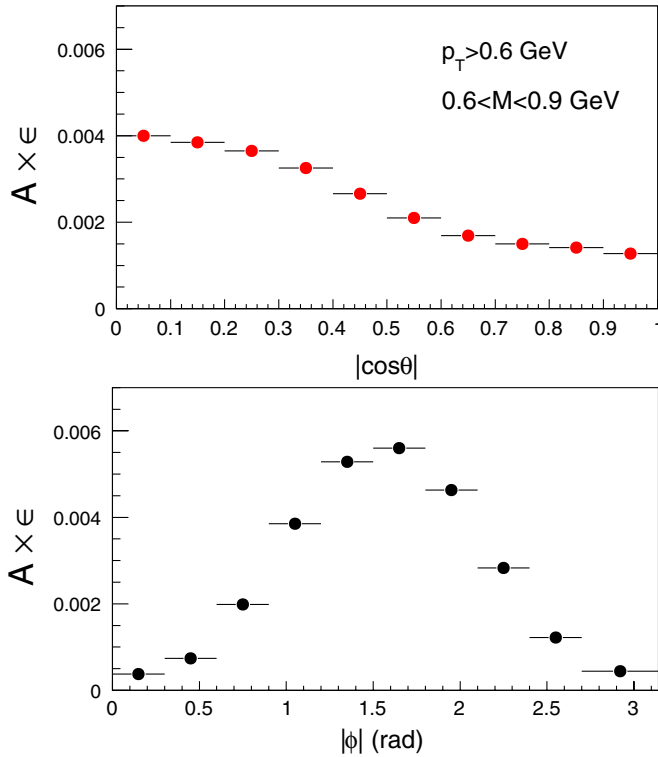


FIG. 2 (color online). Spectrometer acceptance as a function of the two angular variables  $|\cos\theta|$  and  $|\phi|$ .

The rapidity coverage is  $3.2 < y < 4.2$  ( $+0.3 < y_{\text{cm}} < +1.3$ ).

The results on the angular distributions have been analyzed in three different ways, distinguished by the method and the associated statistical or systematic errors. In the first and most rigorous method (1), the 3 structure function parameters  $\lambda$ ,  $\mu$  and  $\nu$  are extracted from a simultaneous fit of the two-dimensional data on the basis of Eq. (1), using a  $6 \times 6$  matrix in the range  $-0.6 < \cos\theta < +0.6$  (bin width 0.2) and  $-0.75 < \cos\phi < 0.75$  (bin width 0.25). The restrictions in range are enforced by regions of very low acceptance in the two-dimensional acceptance matrix, masked in the projections of Fig. 2. The fit values are summarized in Table I for all 4 cases, the two excess mass windows, the  $\omega$  and the  $\phi$ . Within errors, they are all compatible with zero. It is reassuring to see that this is also true for  $\mu$ , as expected for a symmetric collision system at midrapidity on the basis of symmetry considerations [11].

In the second method (2), setting now  $\mu = 0$ , the two-dimensional acceptance-corrected data are projected onto either the  $|\cos\theta|$  or the  $|\phi|$  axis, summing over the two signs. The polar angular distribution is obtained by integrating Eq. (1) over the azimuth angle ( $\phi$ )

$$\frac{dN}{d\cos\theta} = A_0(1 + \lambda\cos^2\theta), \quad (2)$$

while the azimuth angular distribution is obtained by in-

TABLE I. Summary of results for  $p_T > 0.6$  GeV on the structure function parameters  $\lambda$ ,  $\mu$  and  $\nu$  in the CS frame, extracted from three different methods (see text). The  $\chi^2/ndf$  of the fits varies between 0.8 and 1.2. For a cut  $p_T > 1.0$  GeV, the results are the same, within errors.

Excess	$\lambda$	$\nu$	$\mu$
<b><math>0.6 &lt; M &lt; 0.9</math> GeV</b>			
Method 1	$-0.19 \pm 0.12$	$0.03 \pm 0.15$	$0.05 \pm 0.03$
Method 2	$-0.13 \pm 0.12$	$0.05 \pm 0.15$	
Method 3	$-0.15 \pm 0.09$	$0.00 \pm 0.12$	
<b><math>0.4 &lt; M &lt; 0.6</math> GeV</b>			
Method 1	$-0.13 \pm 0.27$	$0.12 \pm 0.30$	$-0.04 \pm 0.10$
Method 2	$-0.10 \pm 0.24$	$0.11 \pm 0.30$	
Method 3	$-0.09 \pm 0.16$	$0.10 \pm 0.18$	
<b><math>\omega</math> meson</b>			
Method 1	$-0.10 \pm 0.10$	$-0.05 \pm 0.11$	$-0.05 \pm 0.02$
Method 2	$-0.12 \pm 0.09$	$-0.06 \pm 0.10$	
Method 3	$-0.12 \pm 0.06$	$-0.02 \pm 0.08$	
<b><math>\phi</math> meson</b>			
Method 1	$-0.07 \pm 0.09$	$-0.10 \pm 0.08$	$0.04 \pm 0.02$
Method 2	$-0.13 \pm 0.08$	$-0.09 \pm 0.08$	
Method 3	$-0.05 \pm 0.06$	$-0.06 \pm 0.06$	

tegration over the polar angle ( $\cos\theta$ )

$$\frac{dN}{d\phi} = A_1 \left( 1 + \frac{\lambda}{3} + \frac{\nu}{3} \cos 2\phi \right). \quad (3)$$

The structure function parameters  $\lambda$  and  $\nu$  can then be determined independently by one-dimensional fits to the respective projections. The data of the polar angular distributions together with the fit lines according to Eq. (2) are shown in Fig. 3 for all four cases, using now 8 bins in  $|\cos\theta|$  (bin width 0.1). The distributions are seen to be uniform, and the fit parameters  $\lambda$ , included in Table I, are again compatible with zero, within errors. To determine the parameter  $\nu$ ,  $\lambda$  [contained in Eq. (3)] is set to the measured value of  $\lambda \pm \sigma_\lambda$ . The fit results for  $\nu$  on the basis of Eq. (3), keeping the small number of bins used in method 1, are again zero, within errors (see Table I).

In the third method (3), the inclusive measured distributions in  $\cos\theta$  and  $\phi$  are analyzed. A one-dimensional acceptance correction is applied in each case, determined by using (as now measured) uniform distributions in  $\phi$  (for  $\cos\theta$ ) and in  $\cos\theta$  (for  $\phi$ ) as an input to the MC simulations. The number of bins in  $|\cos\theta|$  is kept, while that in  $|\phi|$  is increased to 10 (bin width 0.3). The data for the azimuth angular distributions together with the fit lines according to Eq. (3) are shown in Fig. 4. The distributions

are again uniform, as are those for  $\cos\theta$  (not shown, since hardly distinguishable from Fig. 3). The resulting fit parameters for  $\lambda$  and  $\nu$  (taking account again of  $\lambda \pm \sigma_\lambda$ ) are included in Table I. As expected, the errors are smaller than for the other two methods, but the values of  $\lambda$  and  $\nu$  are still close to zero, within errors.

Figures 3 and 4 also contain the systematic errors attached to the individual data points. They mainly arise from two sources. The subtraction of the combinatorial background, with relative uncertainties of 1% [1–3], leads to errors of 2%–3% of the net data for the kinematic selection used here. The subtraction of the meson decay sources causes (correlated) errors for the excess and the vector mesons  $\omega$  and  $\phi$ . With respect to the excess, they range from 4%–6% up to 10%–15% in the low-populated  $\cos\theta - \phi$  matrix bins. This variation is well visible for the overall errors plotted in Figs. 3 and 4. Assuming, very conservatively, these errors to be uncorrelated from point to point, the (statistical) fit errors for  $\lambda$  and  $\nu$  quoted in Table I would increase by 15%–20% if the systematic errors would be added in quadrature. Further confidence into the stability of the results is obtained from their independence of the methods and the bin widths used.

As a completely independent check of the sensitivity of the NA60 set-up to polarization, the  $\eta$  Dalitz decay has also been investigated. Restricting this to the inclusive distribution in  $\cos\theta$ ,  $\lambda = -0.34 \pm 0.05$  is found. This perfectly agrees with the value of  $\lambda = -0.33 \pm 0.05$  determined by a Monte Carlo simulation, taking account of the kinematic distributions of the  $\eta$  in  $M$  and  $p_T$  and assuming a  $(1 + \cos^2\theta)$  distribution in the internal decay frame.

The global outcome from our analysis of the excess-dimuon angular distributions is straightforward: the structure function parameters  $\lambda$ ,  $\mu$  and  $\nu$  are all zero within the statistical and systematic errors, and the projected distributions in polar and azimuth angle are all uniform. This applies not only for the excess dileptons as anticipated if of thermal origin, but also for the vector mesons  $\omega$  and  $\phi$ . While there may be a rather direct connection between the two findings in nuclear collisions, it is of interest to note that the result of  $\lambda = 0$  has been reported before for  $\rho$  and  $\omega$  production in  $p - p$  [16] and  $\pi^- - C$  [17].

We conclude, following the primary motivation of this study, that the absence of any polarization is fully consistent with the interpretation of the observed excess dimuons as thermal radiation from a randomized system. While this

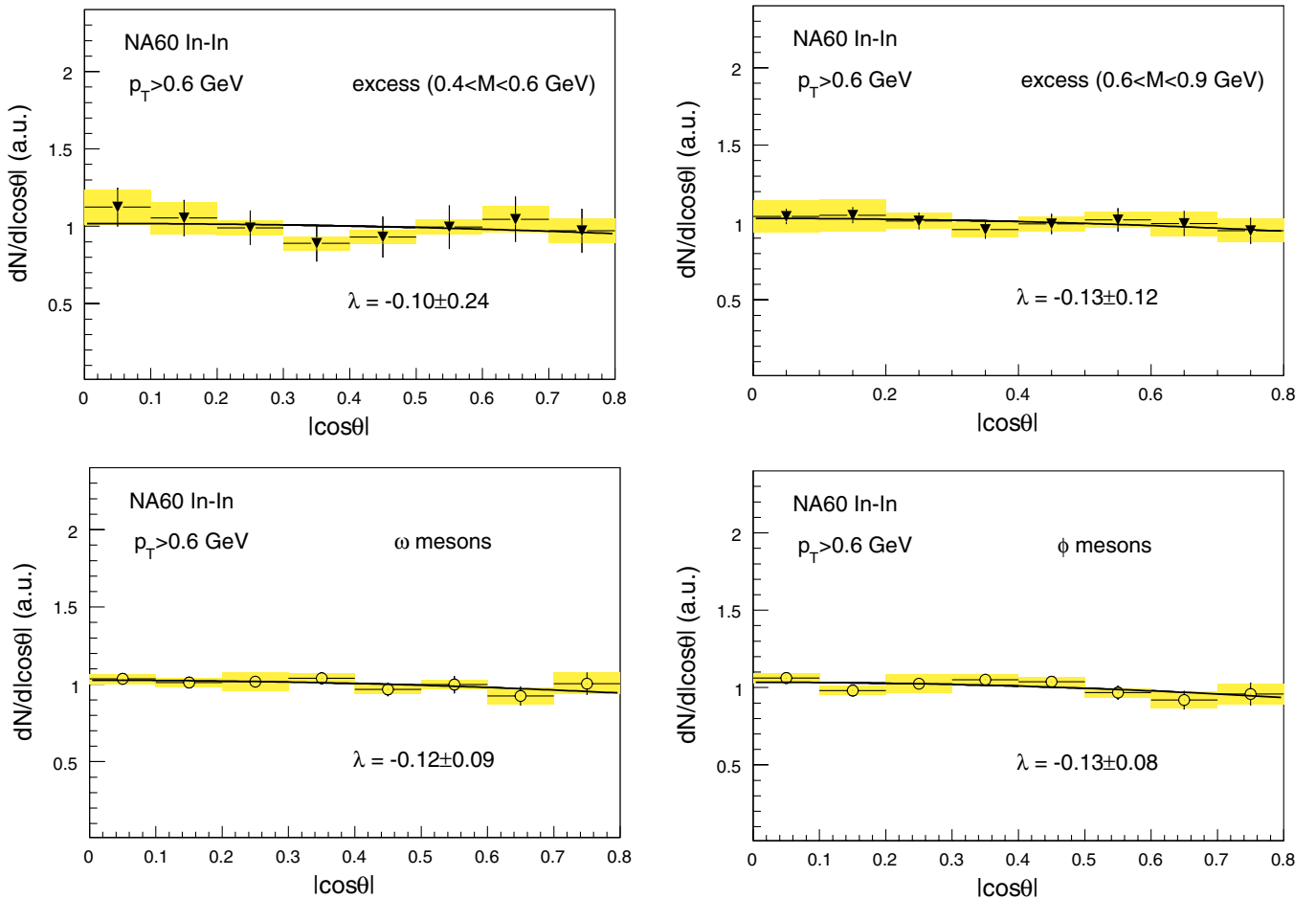


FIG. 3 (color online). Polar angle distributions of excess dileptons and of the vector mesons  $\omega$  and  $\phi$ .

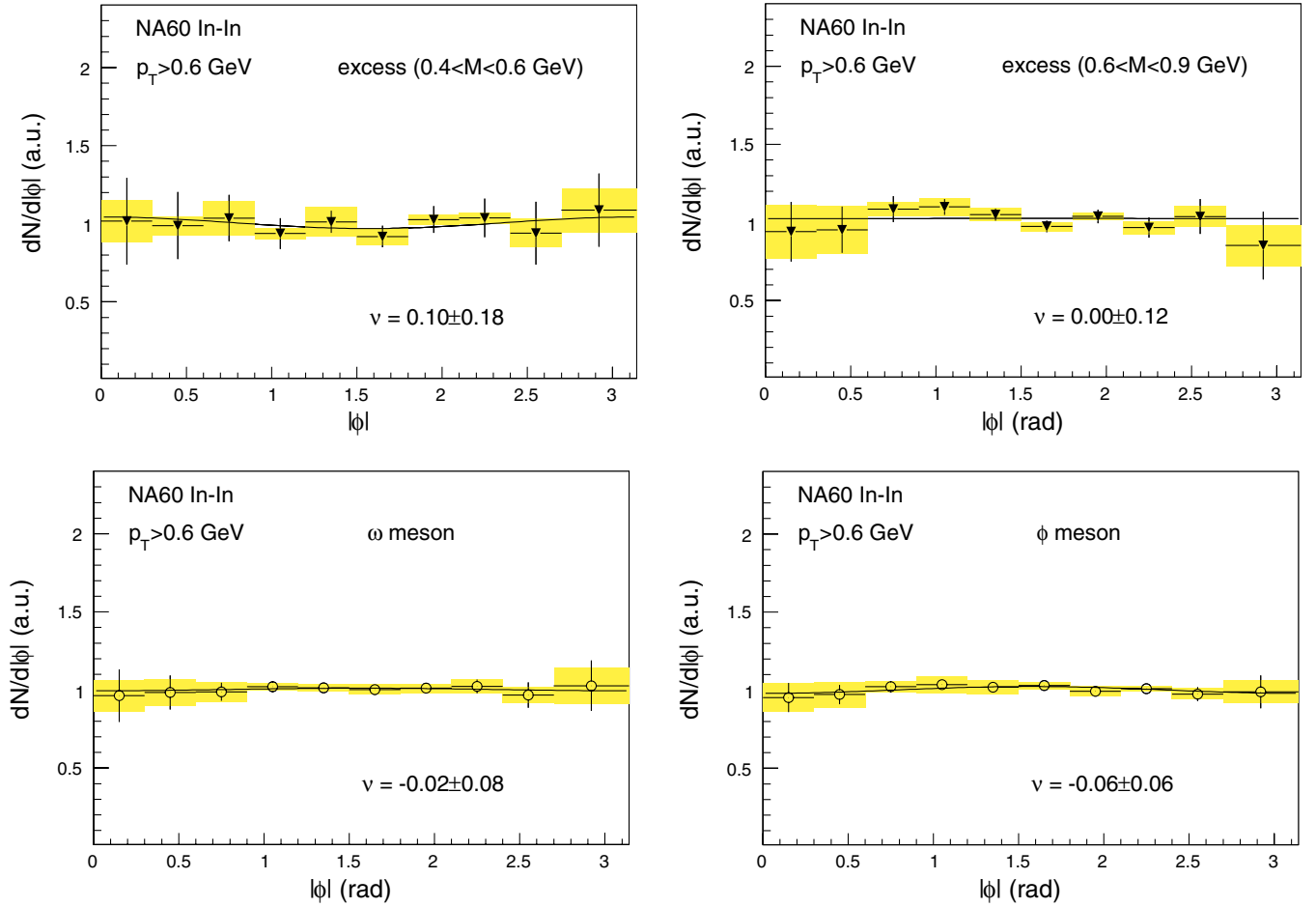


FIG. 4 (color online). Azimuth angle distributions of excess dileptons and of the vector mesons  $\omega$  and  $\phi$ .

is a necessary condition, it is not sufficient. However, together with other features like the Planck-like shape of the excess mass spectra [3,18], the exponential shape of the  $m_T$  spectra [2,18] and the global agreement with theoretical models both as to spectral shapes and absolute yields [3,18], the thermal interpretation is now based on increasingly solid grounds.

We are grateful to O. Nachtmann for useful discussions.

- 
- [1] R. Arnaldi *et al.* (NA60 Collaboration), Phys. Rev. Lett. **96**, 162302 (2006).  
 [2] R. Arnaldi *et al.* (NA60 Collaboration), Phys. Rev. Lett. **100**, 022302 (2008).  
 [3] R. Arnaldi *et al.* (NA60 Collaboration), Eur. Phys. J. C **59**, 607 (2009).  
 [4] S. D. Drell and T. M. Yan, Phys. Rev. Lett. **25**, 316 (1970).  
 [5] J. C. Collins and D. E. Soper, Phys. Rev. D **16**, 2219 (1977).  
 [6] C. S. Lam and W. K. Tung, Phys. Rev. D **18**, 2447 (1978).

- [7] J. Badier *et al.* (NA3 Collaboration), Z. Phys. C **11**, 195 (1981).  
 [8] S. Falciano *et al.* (NA10 Collaboration), Z. Phys. C **31**, 513 (1986); M. Guanziroli *et al.* (NA10 Collaboration), Z. Phys. C **37**, 545 (1988).  
 [9] K. Gottfried and J. D. Jackson, Nuovo Cimento **33**, 309 (1964).  
 [10] A. Brandenburg, O. Nachtmann, and E. Mirkes, Z. Phys. C **60**, 697 (1993); D. Boer, A. Brandenburg, O. Nachtmann, and A. Utermann, Eur. Phys. J. C **40**, 55 (2005).  
 [11] O. Nachtmann (private communication).  
 [12] E. L. Bratkovskaya, O. V. Teryaev, V. D. Toneev, Phys. Lett. B **348**, 283 (1995).  
 [13] P. Hoyer, Phys. Lett. B **187**, 162 (1987).  
 [14] K. Banicz *et al.*, Nucl. Instrum. Methods Phys. Res., Sect. A **546**, 51 (2005).  
 [15] S. Damjanovic *et al.*, Nucl. Phys. A **783**, 327 (2007).  
 [16] V. Blobel *et al.*, Phys. Lett. B **48**, 73 (1974).  
 [17] J. G. Branson *et al.*, Phys. Rev. Lett. **38**, 1331 (1977).  
 [18] R. Arnaldi *et al.* (NA60 Collaboration), arXiv:0812.3053 [Eur. Phys. J. C (to be published)].